Int. J. Electrochem. Sci., 12 **(2017)** 10369 – 10380, doi: 10.20964/2017.11.88

International Journal of
ELECTROCHEMICAL
SCIENCE
www.electrochemsci.org

Electrochemical Investigations of the Inhibitive Activity of a Pyridazinium Ionic Liquid for the Acid Corrosion of Carbon Steel

Sami BEN AOUN

Department of Chemistry, Faculty of Science, Taibah University, PO. Box 30002 Al Madinah Al Munawarah, KSA.
E-mail: sbenaoun@taibahu.edu.sa

Received: 22 August 2017 / *Accepted:* 23 September 2017 / *Published:* 12 October 2017

A1-benzylpyridazin-1-ium bromide inhibition of the corrosion of carbon steel in molar hydrochloric acid has been investigated by electrochemical methods. MS20 adsorbed onto both hydrogen reduction and carbon steel dissolution active sites and acted as mixed-type inhibitor. The increasing MS20 concentrations induced increasing surface coverage and inhibition efficiency as concluded from both linear polarization and electrochemical impedance spectroscopy. In the former, a decreasing corrosion current and a positive corrosion potential shift were observed. While, in the latter, it led to an increasing charge transfer resistance and a decreasing double layer capacitance. The formation of a protective film was confirmed by SEM.

Keywords: Carbon steel; Corrosion; Ionic liquids; Linear polarization; Electrochemical impedance spectroscopy; Adsorption.

1. INTRODUCTION

The electrochemical dissolution of reactive metals is raising increasing economical and health concerns [1, 2] especially with the excessive industrial use of acids viz. hydrochloric acid in particular [3, 4] which causes the corrosive damage of various metals, specifically carbon steel that is commonly regarded as one of the most widely used engineering materials [5].This explains the great deal of work focusing on the use of corrosion inhibitors, mostly organic compounds [6-12], aiming at controlling this unavoidable problem. The most effective reported corrosion inhibitors were those containing aromatic rings and heteroatoms [13-21] owing to their relatively strong adsorption onto metal surface

[22, 23]. At a later stage, tremendous efforts have been deployed to overcome the hazardous nature of most organic inhibitors affecting both the human being and the environment.

Recently, a rising interest has been paid to ionic liquids as a new class of eco-friendly corrosion inhibitors [24-30]. These wonder compounds, mostly existing in liquid state at room temperature [31, 32], are excellent solvents so much so that they were considered as solvents of the future [33].

Ionic liquids typically comprises an organic cation and a complex anion holding together electrostatically [34]. They are endowed with a negligible vapor pressure, excellent ionic conductivity and high thermal stability [35-38]. Very promising results were reported for the corrosion inhibition activities of ionic liquids particularly for aluminum [39], copper [40, 41] and carbon steel [25, 42-44].

The present paper presents the electrochemical assessment, using linear polarization and electrochemical impedance spectroscopy techniques, of the corrosion inhibition of carbon steel in hydrochloric acid media with a pyridazinium ionic liquid. The obtained results will be correlated with those obtained previously by chemical method [45] aiming at confirming the adsorptive characteristics of the investigated ionic liquid, elucidating the various reactions kinetics and characterizing the interfacial double layer during the corrosion inhibition process. Surface morphologies will be studied by scanning electron microscopy.

2. MATERIALS AND METHODS

2.1.Chemicals:

Scheme 1 displays the chemical structure of the ionic liquid investigated in the present study that will be designated as (MS20) in the text. Hydrochloric acid (37%) and acetone (99.5%) were obtained from Panreac and ethanol (99.8%) was purchased from Sigma-Aldrich. The corrosive media was prepared by proper dilution of the acid stock solution using distilled water and when necessary, the appropriate amount of MS20 compound was dissolved in the corrosive media.

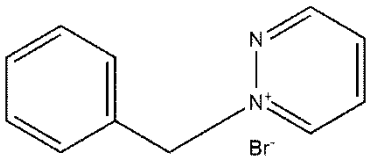

Scheme 1. Chemical structure of 1-benzylpyridazin-1-ium bromide (MS20).

2.2. Materials:

The test samples were prepared by cutting cylinders of 1 cm^2 cross-sectional area from a pre-treated half-millimeter thick carbon steel sheet. The pre-treatment consisted of cleaning and degreasing then mechanical polishing to a mirror-like appearance. The samples were then cleaned thoroughly with

subsequent copious amounts of acetone, ethanol and distilled water then dried and kept in a desiccator for electrochemical experiments.

2.3. Electrochemical measurements

The as-prepared specimen was fitted into a Teflon sample holder and served as the working electrode, in connection with a saturated calomel electrode (SCE) reference electrode and two platinum-sheet counter electrodes. In order to minimize to ohmic drop, the reference electrode tip was brought very close to the working electrode surface by means of a Luggin capillary. The electrolytic solution volume was maintained constant at 500 mL in all experiments and the test samples were immersed for 30 min before measurements to attain a steady open circuit potential. A potentiostat/galvanostat (PGSTAT 128N, Metrohm Autolab B.V, The Netherlands) controlled by NOVA 2.1 software was used to carry out and analyze all the experiments.

For polarization measurements, the potential was scanned at a rate of 1 $mV.s^{-1}$ with a step potential of 1 mV and the potential range was ± 100 mV with respect to the corrosion potential.

As for the electrochemical impedance spectroscopy experiments, the frequency response at the open circuit potential between 0.1 MHz and 0.5 Hz was analyzed using the built-in frequency response analyzer (FRA23M) following a single sine wave perturbation with 10 mV amplitude and an integration time of 125 ms.

All experiments were carried out at room temperature (i.e 296 K).

2.4. Surface characterization:

Scanning electron microscopy was carried out by means of a JCM-6000 NeoScope (Jeol, Japan) operating at 15 kV under a high vacuum condition. This permits the monitoring of the corroding metal surface in the successive corrosive media

3. RESULTS AND DISCUSSION

3.1. Linear Polarization:

Fig.1 displays the voltammograms obtained from linear polarization experiments related to the corrosion tests of carbon-steel samples in the presence of various concentrations (i.e. $0\text{-}10^{-3}$ M) of MS20 compound in 1M HCl solution. The general shape reveals that both anodic and cathodic reactions are activation-controlled [46, 47] rendering it possible to use the Tafel extrapolation method in order to extract relevant electrochemical parameters from both branches. For instance, the anodic and cathodic constants (β_a and β_c, respectively) as well as the respective corrosion current and potential (i.e. I_{corr} and E_{corr}) are shown in Table 1.

The quasi-identical shapes of Fig. 1 curves indicate the invariance of both red-ox processes upon addition of MS20 at various concentrations [48]. In addition, the decreasing cathodic and anodic

currents in the presence of the studied ionic liquid infer a dual control of both cathodic and anodic corrosion reactions [49] though this decrease is much clearly pronounced for the anodic branches of the voltammograms revealing a predominantly anodic reaction inhibition. The nearly-parallel Tafel lines for both processes confirmed by the slightly modified values of cathodic and anodic slopes as presented in Table 1 give an indication that the MS20 inhibition of the corrosion of carbon steel works through the simultaneous blocking of anodic and cathodic reactions active sites [50, 51].

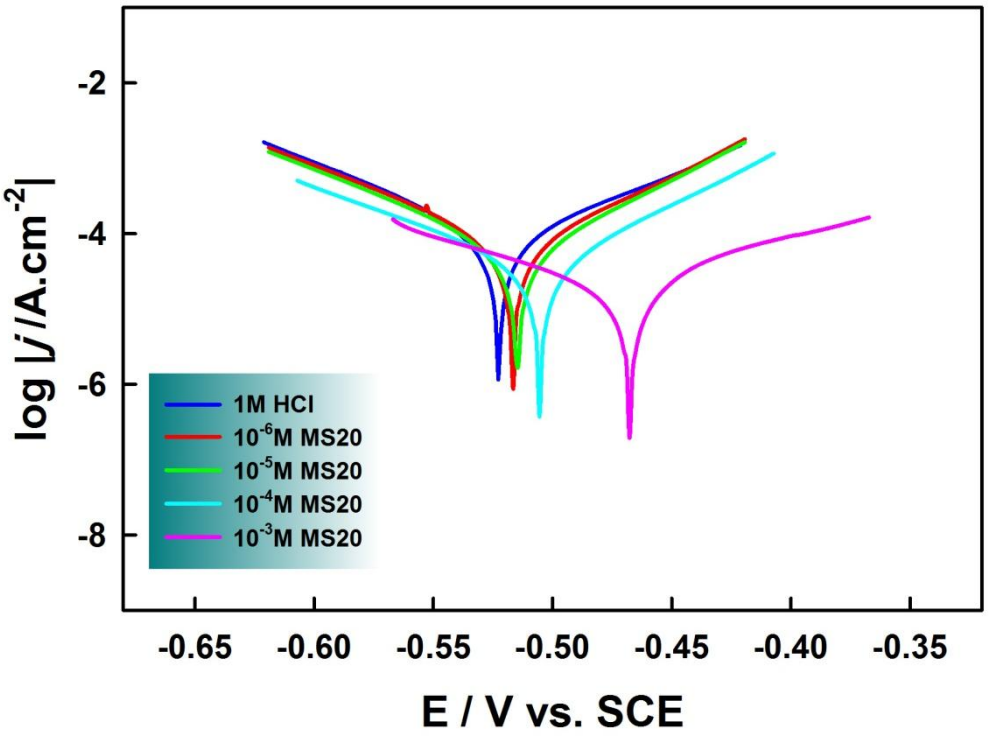

Figure 1. Carbon steel linear polarization curves in 1 M HCl with different concentrations of MS20.

On the other hand, the corrosion potential was affected by the addition of MS20 and the maximal change observed at [MS20] = 10^{-3} M being inferior to 85 mV indicates the mixed-type inhibitive activity of this compound [52] with a slightly dominating anodic nature as the shift was towards more positive potential values in the investigated concentration range [49].

The inhibition efficiency of MS20 for carbon steel corrosion is directly related to the corrosion current density and can therefore be calculated by the equation [53]:

$$IE\% = \frac{I^0_{corr} - I_{corr}}{I^0_{corr}} \times 100 \quad (1)$$

(IE%) is the inhibition efficiency, I^0_{corr} is the corrosion current density in the absence of inhibitor and I_{corr} the one in its presence.

In the present work, a steady increase of the (IE%) values with increasing [MS20] is observed which attained ca. 84% in the presence of 10^{-3} M MS20 (cf. Table 1) in a very good agreement with the similar trend reported using weight-loss method [45]. This observation favors again the adsorption of the ionic liquid molecules onto the interface of the corroding metal and the corrosive electrolyte

[54] leading to an increasing coverage (θ) of the carbon steel surface when the inhibitor's concentration is increased, as can be calculated from the equation [51]:

$$\theta = 1 - \frac{I_{corr}}{I^0_{corr}} \quad (2)$$

And that confirms again the blocking effect of the corrosion active sites exerted by the adsorbed ionic liquid molecules [52].

Table 1. Carbon steel linear polarization parameters in 1 M HCl with different concentrations of MS20

[MS20] ($mol.L^{-1}$)	E_{corr} (mV)	I_{corr} ($A.cm^{-2}$)	β_a ($mV.dec^{-1}$)	$-\beta_c$ ($mV.dec^{-1}$)	IE %	θ
Blank	-523	1.14E-04	104	86	---	---
10^{-6}	-517	8.59E-05	83	85	24.4	0.244
10^{-5}	-515	5.44E-05	63	80	52.1	0.521
10^{-4}	-505	4.16E-05	71	96	63.4	0.634
10^{-3}	-468	1.82E-05	110	97	84.0	0.840

In view of these results, the investigated MS20 compound shows an effective inhibition of the carbon steel corrosion through the simultaneous retardation of the cathodic reduction process of hydrogen and of the kinetic hindering of the anodic dissolution of the corroding metal. It is noteworthy that the obtained inhibition efficiency is far higher than several reported data in literature as shown in table 2.

Table 2. Comparison of carbon steel corrosion inhibition efficiencies from reported results in literature against the current investigation based on polarization parameters.

Corrosive media	Inhibitor	Concentration (M)	IE %	Reference
1M HCl	HMDTMPA	1E-3	70.6	[1]
0.5 M HCl	HMDTMP	1E-3	84.0	[48]
5% HCl	mimosa tannin	1E-3	66.2	[51]
1M HCl	DIT	1E-3	75.0	[55]
1M HCl	DNSO	1E-3	69.1	[56]
1M HCl	cloxacillin	1E-3	69.4	[57]
1M HCl	IL I	1E-3	64.3	[58]
	IL II	1E-3	62.0	
	IL III	1E-3	74.0	
	IL IV	1E-3	63.8	
1M HCl	BT39	1E-3	55.0	[59]
	BT40	1E-3	78.0	
1M HCl	GP2	1E-3	83.9	[60]
1M HCl	MS20	1E-3	84.0	This work

3.2.Electrochemical Impedance Spectroscopy:

The electrochemical impedance spectroscopy results are given as Nyquist and Bode plots in Fig. 2 and Fig. 3, respectively. The single capacitive loop shown in Fig. 2 confirmed by the single maximum phase angle in Fig. 3b implies the activation-controlled process of carbon steel corrosion [23] both in the absence and presence of inhibiting MS20 compound which supports the polarization results discussed in the previous section. The corrosion mechanism didn't change in the presence of inhibitor since the semicircles of Fig. 2 have generally similar shapes [61].

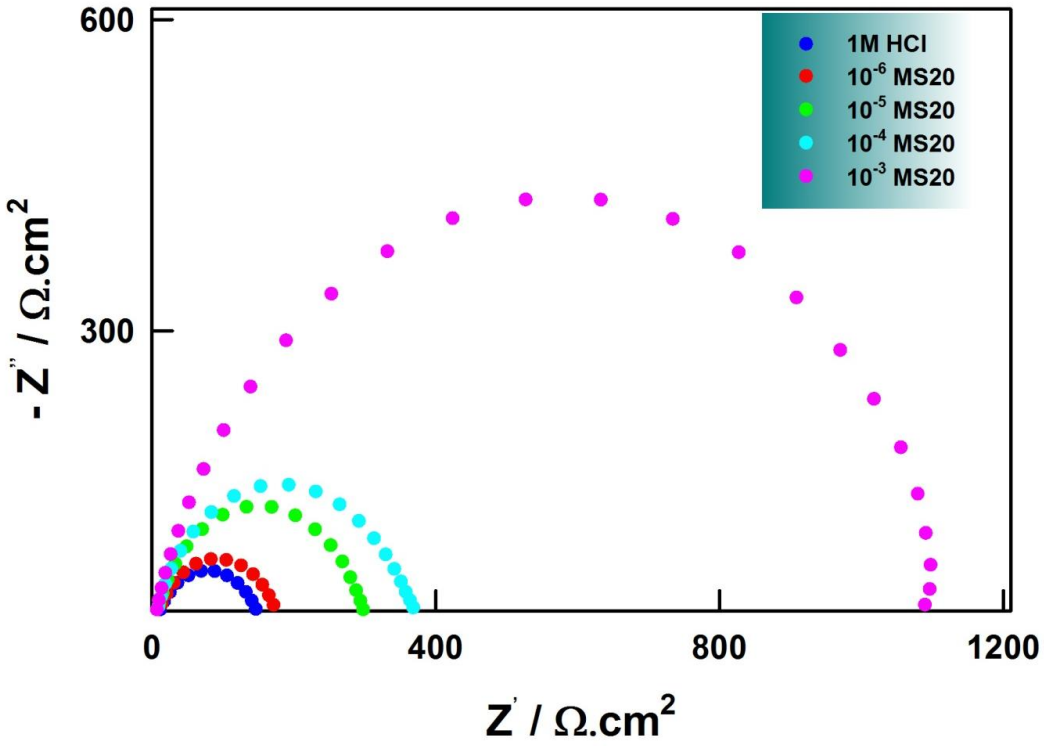

Figure 2. Carbon steel Nyquist plots in 1 M HCl with different concentrations of MS20.

The electrical circuit used to fit the impedance data is shown in Fig. 4 where R_{ct} and R_s represent respectively, the charge transfer resistance and solution resistance. CPE represents the double layer impedance and the introduction of a constant phase element comes in replacement for a pure double layer capacitance for accuracy of fitting results [62] since the capacitive loops of Fig. 2 have the shapes of depressed semicircles which is shown in Bode plots as slopes' absolute values differing from unity (sloping lines of Fig. 3a) as a consequence of the frequency dispersion effects caused by surface irregularities which are generally attributed to surface roughness and inhomogeneity [63].

The charge transfer resistance remarkable increase (cf. Table 3) is clearly noticeable from the increasing diameters of the capacitive loops in Fig. 2 and that is explainable by the formation of an insulating protective film onto the corroding metal surface [23, 61] which by consequence leads to increasing inhibition efficiency as shown in Table 3 reaching ca. 85.7% in the presence of 1mM MS20 compound in a very good agreement with the polarization measurements.

Table 3. Carbon steel Electrochemical impedance spectroscopy parameters in 1 M HCl with different concentrations of MS20

[MS20] ($mol.L^{-1}$)	R^0_{ct} ($\Omega.cm^2$)	R_{ct} ($\Omega.cm^2$)	IE%	θ	Y_0 ($Mho.cm^{-2}$)	n	C_{dl} ($F.cm^{-2}$)
Blank	158.1	158.1	…	…	5.29E-05	9.22E-01	3.54E-05
10^{-6}	158.1	184.4	14.3	0.143	6.06E-05	9.13E-01	3.96E-05
10^{-5}	158.1	306.5	48.4	0.484	5.25E-05	9.01E-01	3.34E-05
10^{-4}	158.1	382.0	58.6	0.586	5.94E-05	8.49E-01	3.03E-05
10^{-3}	158.1	1102.6	85.7	0.857	2.76E-05	8.49E-01	1.48E-05

The inhibition efficiency in this case is calculated using the values of charge transfer resistance in the absence (R^0_{ct}) and presence (R_{ct}) of inhibitor according to the following equation [64]:

$$IE\% = \frac{R^0_{ct} - R_{ct}}{R^0_{ct}} \times 100 \quad (3)$$

Obviously, the growing protective film reduces the exposed carbon steel surface and increases its surface coverage (θ) which is given by the equation:

$$\theta = \frac{R^0_{ct} - R_{ct}}{R^0_{ct}} \quad (4)$$

The impedance of the constant phase element with (Y_0) value and (n) exponent used to fit the electrochemical impedance spectra presenting and angular frequency (w) obeys the equation [65]:

$$Z_{CPE} = \frac{1}{Y_0(jw)^n} \quad (5)$$

The exponent (n) gives an indication of the degree of surface irregularities, for instance n=1 for a perfectly homogeneous surface that will act as a perfect capacitor [51]. j is the square root of (−1).

Fig. 3a reveals the impedance increase with increasing MS20 concentration as a consequence of decreasing corrosion rate, supporting again the inhibiting activity of the investigated compound.

The double layer capacitance values can be calculated from the constant phase element parameters using the equation [48]:

$$C_{dl} = \sqrt[n]{Y_0 R_{ct}^{1-n}} \quad (6)$$

The double layer capacitance follows the opposite trend of the charge transfer resistance with decreasing values as a consequence of increasing inhibitor concentration and that is attributable to the displacement of water molecules from the corroding metal surface and their replacement with adsorbed inhibitor molecules [47, 48, 61] which agrees well with the polarization results. Such adsorption reduces the double layer capacitance as per the equation [66]:

$$C_{dl} = \frac{\varepsilon_0 \times \varepsilon_r}{\delta} \quad (7)$$

(δ) is the thickness of the insulating film, (ε_0) and (ε_r) are the vacuum and the corrosive media permittivities, respectively.

Another indication of the inhibitory effect of the investigated compound shown in Fig. 3b is the increasing maximum phase angle with increasing concentration of MS20 compound reaching ~ ca. −80° in the presence of [MS20] = 10^{-3} M which approaches the ideal capacitor's phase shift (i.e. −90°) [61] confirming the formation of a protective layer the thickness of which increased with increasing MS20 concentration which is also evidenced by the broadening of the maximum phase angle [47].

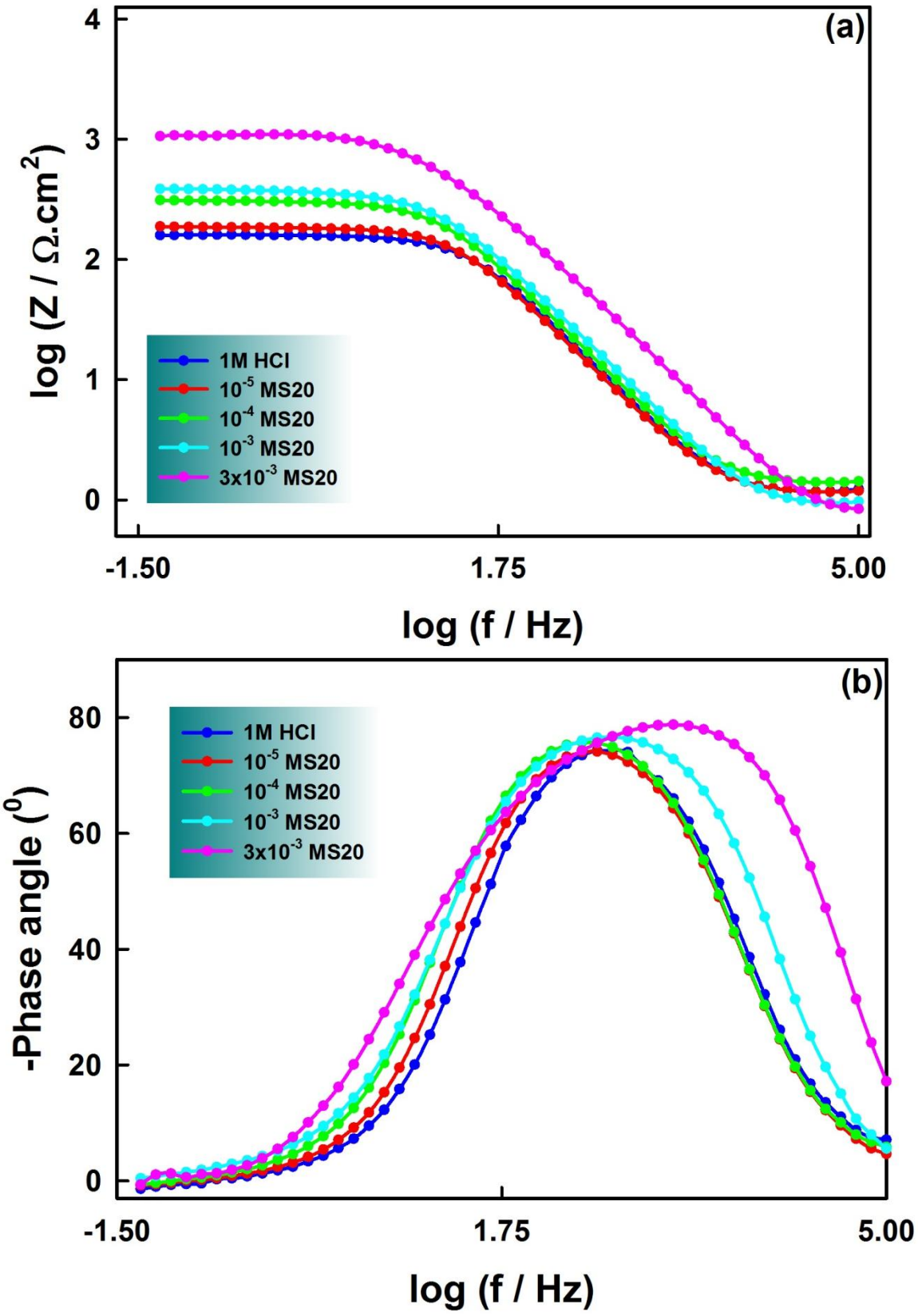

Figure 3. Carbon steel Bode plots in 1 M HCl with different concentrations of MS20.

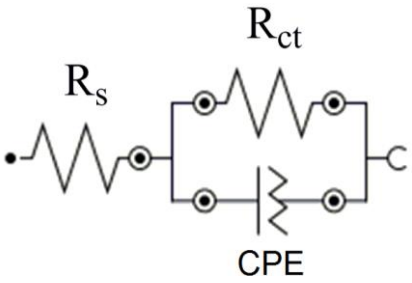

Figure 4. Electrochemical impedance spectroscopy data analysis equivalent circuit.

3.3.Scanning electron microscopy:

Inspection of the SEM micrographs displayed in Fig. 5 shows that exposing carbon steel surface to 1M HCl led to its excessive damage (Fig. 5a).

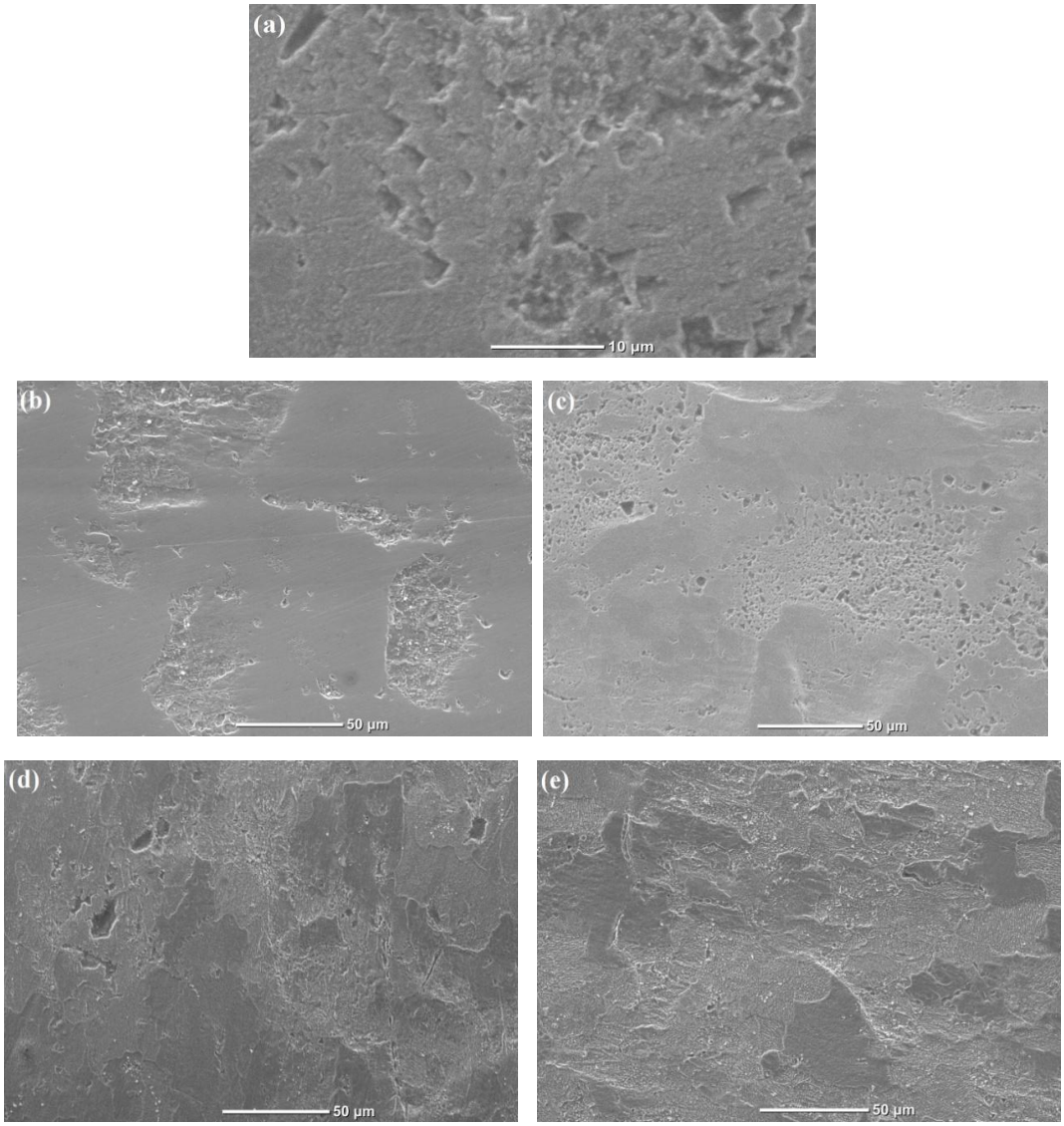

Figure 5. SEM micrographs after 5 hours exposure at 296 K of carbon steel specimens in 1 M HCl containing (a) 0 M (b) 10^{-6} M, (c) 10^{-5} M, (d) 10^{-4} M and (e) 10^{-3} M MS20.

A clearly reduced damage is observed upon addition of 10^{-6} M MS20 as shown in Fig. 5b. The film defects decreased with increasing MS20 concentration (cf. Figs. 5b-5e) which supports the increasing surface coverage concluded from the electrochemical study results.

Additionally, a noticeable increase in the protective film thickness is evidenced in the presence of 1 mM MS20 as can be seen in Fig. 5e which agrees very well with the pronounced decrease of the double layer capacitance (i.e. 14.8 $\mu F.cm^{-2}$) reported in Table 3.

4. CONCLUSION

Carbon steel corrosion in 1M HCl has been investigated by electrochemical techniques in the presence of MS20 ionic liquid at room temperature. The linear polarization measurements revealed that both hydrogen evolution and metal dissolution reactions are activation-controlled whether in the presence or absence of the investigated ionic liquid. A dual control of both reactions was shown in the presence of MS20 with a predominant anodic effect and the inhibition proceeds through the blocking of both reactions' active sites as a consequence of its strong adsorption onto the metal surface. The corrosion potential shift inferred that MS20 acted as a mixed-type inhibitor. The electrochemical impedance spectroscopy confirmed the single charge-transfer control of the metal corrosion process and its non-alteration in the presence of inhibitor. The variation of charge transfer resistance with MS20 concentration proved the formation of an insulating protective film with a growing thickness with rising inhibitor's concentration as depicted from the calculated double layer capacitance values. The inhibition efficiencies reached a maximum in the presence of 10^{-3} M MS20 with very close values (i.e. ca. 84.0% and ca. 85.7%) for both techniques (i.e. polarization and electrochemical impedance spectroscopy, respectively). The scanning electron microscopy revealed the formation of a growing protecting film the thickness of which increased with increasing MS20 concentrations which corroborates very nicely with the electrochemical study results.

References

1. M.R. Laamari, J. Benzakour, F. Berrekhis, A. Derja, D. Villemin, *Arab. J. Chem.*, 9, Supplement 1 (2016) S245-S251.
2. S. Kharchouf, L. Majidi, M. Bouklah, B. Hammouti, A. Bouyanzer, A. Aouniti, *Arab. J. Chem.*, 7 (2014) 680-686.
3. I. Ahamad, R. Prasad, M.A. Quraishi, *Corros. Sci.*, 52 (2010) 3033-3041.
4. A.H. Al Hamzi, H. Zarrok, A. Zarrouk, R. Salghi, B. Hammouti, S.S. Al-Deyab, M. Bouachrine, A. Amine, F. Guenoun, *Intern. J. ELectrochem. Sci.*, 8 (2013) 2586-2605.
5. S. Ben Aoun, M. Bouklah, K.F. Khaled, B. Hammouti, *Intern. J. ELectrochem. Sci.*, 11 (2016) 7343-7358.
6. S. Zheng, J. Li, *J. Sol-Gel Sci. Technol.*, 54 (2010) 174-187.
7. A.C. Balaskas, I.A. Kartsonakis, D. Snihirova, M.F. Montemor, G. Kordas, *Progress in Organic Coatings*, 72 (2011) 653-662.
8. S.A.S. Dias, S.V. Lamaka, C.A. Nogueira, T.C. Diamantino, M.G.S. Ferreira, *Corros. Sci.*, 62

(2012) 153-162.
9. S. Peng, W. Zhao, H. Li, Z. Zeng, Q. Xue, X. Wu, *Appl. Surf. Sci.*, 276 (2013) 284-290.
10. E. Roussi, A. Tsetsekou, A. Skarmoutsou, C.A. Charitidis, A. Karantonis, *Surf. Coat. Technol.*, 232 (2013) 131-141.
11. I. Santana, A. Pepe, E. Jimenez-Pique, S. Pellice, I. Milošev, S. Ceré, *Surf. Coat. Technol.*, 265 (2015) 106-116.
12. M. Yu, M. Liang, J. Liu, S. Li, B. Xue, H. Zhao, *Appl. Surf. Sci.*, 363 (2016) 229-239.
13. K.R. Ansari, M.A. Quraishi, A. Singh, *Measurement*, 76 (2015) 136-147.
14. M. Yadav, S. Kumar, U. Sharma, P.N. Yadav, *J. Mater. Environ. Sci.*, 4 (2013) 691-700.
15. K.R. Ansari, Sudheer, A. Singh, M.A. Quraishi, *J. Dispersion Sci. Technol.*, 36 (2015) 908-917.
16. N. Caliskan, E. Akbas, *Mater. Chem. Phys.*, 126 (2011) 983-988.
17. X. Li, X. Xie, S. Deng, G. Du, *Corros. Sci.*, 87 (2014) 27-39.
18. A.O. Yüce, G. Kardaş, *Corros. Sci.*, 58 (2012) 86-94.
19. M.A. Chidiebere, E.E. Oguzie, L. Liu, Y. Li, F. Wang, *Mater. Chem. Phys.*, 156 (2015) 95-104.
20. M. Finšgar, D. Kek Merl, *Corros. Sci.*, 83 (2014) 164-175.
21. S. Hari Kumar, S. Karthikeyan, *J. Mater. Environ. Sci.*, 4 (2013) 675-684.
22. S. Ben Aoun, *Der Pharma Chemica*, 5 (2013) 294-304.
23. H. Lgaz, R. Salghi, S. Jodeh, B. Hammouti, *J. Mol. Liq.*, 225 (2017) 271-280.
24. Q. Zhang, Y. Hua, *Mater. Chem. Phys.*, 119 (2010) 57-64.
25. N.V. Likhanova, M.A. Domínguez-Aguilar, O. Olivares-Xometl, N. Nava-Entzana, E. Arce, H. Dorantes, *Corros. Sci.*, 52 (2010) 2088-2097.
26. X. Zhou, H. Yang, F. Wang, *Electrochim. Acta*, 56 (2011) 4268-4275.
27. M. Scendo, J. Uznanska, *International Journal of Corrosion*, 2011 (2011).
28. P. Huang, J.-A. Latham, D.R. MacFarlane, P.C. Howlett, M. Forsyth, *Electrochim. Acta*, 110 (2013) 501-510.
29. X. Zheng, S. Zhang, W. Li, M. Gong, L. Yin, *Corros. Sci.*, 95 (2015) 168-179.
30. I. Lozano, E. Mazario, C.O. Olivares-Xometl, N.V. Likhanova, P. Herrasti, *Mater. Chem. Phys.*, 147 (2014) 191-197.
31. N. Jain, A. Kumar, S. Chauhan, S.M.S. Chauhan, *Tetrahedron*, 61 (2005) 1015-1060.
32. J.S. Wilkes, *Green Chemistry*, 4 (2002) 73-80.
33. R.D. Rogers, K.R. Seddon, *Science*, 302 (2003) 792-793.
34. M. Messali, *J. Mater. Environ. Sci.*, 2 (2011) 174-185.
35. H.L. Ngo, K. LeCompte, L. Hargens, A.B. McEwen, *Thermochim. Acta*, 357-358 (2000) 97-102.
36. P. Bonĥte, A.P. Dias, N. Papageorgiou, K. Kalyanasundaram, M. Grätzel, *Inorg. Chem.*, 35 (1996) 1168-1178.
37. S.A. Forsyth, J.M. Pringle, D.R. MacFarlane, *Australian Journal of Chemistry*, 57 (2004) 113-119.
38. F. Endres, S. Zein El Abedin, *Phys. Chem. Chem. Phys.*, 8 (2006) 2101-2116.
39. M.A. Quraishi, M.Z.A. Rafiquee, S. Khan, N. Saxena, *J. Appl. Electrochem.*, 37 (2007) 1153-1162.
40. R. Gašparac, C.R. Martin, E. Stupnišek-Lisac, *J. Electrochem. Soc.*, 147 (2000) 548-551.
41. D.Q. Zhang, L.X. Gao, G.D. Zhou, *Corros. Sci.*, 46 (2004) 3031-3040.
42. S. Muralidharan, S. Venkatakrishna Iyer, *Anti-Corros. Meth. Mater.*, 44 (1997) 100-106.
43. S. Shi, P. Yi, C. Cao, X. Wang, J. Su, J. Liu, *Huagong Xuebao/Journal of Chemical Industry and Engineering (China)*, 56 (2005) 1112-1119.
44. Q.B. Zhang, Y.X. Hua, *Electrochim. Acta*, 54 (2009) 1881-1887.
45. S. Ben Aoun, *Intern. J. ELectrochem. Sci.*, 8 (2013) 10788-10804.
46. S. Issaadi, T. Douadi, A. Zouaoui, S. Chafaa, M.A. Khan, G. Bouet, *Corros. Sci.*, 53 (2011) 1484-1488.
47. K.R. Ansari, M.A. Quraishi, A. Singh, S. Ramkumar, I.B. Obote, *RSC Advances*, 6 (2016) 24130-24141.
48. R. Laamari, J. Benzakour, F. Berrekhis, A. Abouelfida, A. Derja, D. Villemin, *Arab. J. Chem.*, 4

(2011) 271-277.
49. H.-h. Zhang, K. Gao, L. Yan, X. Pang, *J. Electroanal. Chem.*, 791 (2017) 83-94.
50. M. Parveen, M. Mobin, S. Zehra, *RSC Advances*, 6 (2016) 61235-61248.
51. S. Martinez, M. Metikoš-Huković, *J. Appl. Electrochem.*, 33 (2003) 1137-1142.
52. L. Fragoza-Mar, O. Olivares-Xometl, M.A. Domínguez-Aguilar, E.A. Flores, P. Arellanes-Lozada, F. Jiménez-Cruz, *Corros. Sci.*, 61 (2012) 171-184.
53. S.K. Shukla, A.K. Singh, I. Ahamad, M.A. Quraishi, *Mater. Lett.*, 63 (2009) 819-822.
54. M.R. laamari, J. Benzakour, F. Berrekhis, M. Bakasse, D. Villemin, *Arab. J. Chem.*, 9, Supplement 2 (2016) S1218-S1224.
55. D. Ben Hmamou, M.R. Aouad, R. Salghi, A. Zarrouk, M. Assouag, O. Benali, M. Messali, H. Zarrok, B. Hammouti, *J. Chem. Pharm. Res.*, 4 (2012) 3489-3497.
56. L. Afia, N. Rezki, M.R. Aouad, A. Zarrouk, H. Zarrok, R. Salghi, B. Hammouti, M. Messali, S.S. Al-Deyab, *Intern. J. ELectrochem. Sci.*, 8 (2013) 4346-4360.
57. S. Hari Kumar, S. Karthikeyan, *J. Mater. Environ. Sci.*, 3 (2012) 925-934.
58. M.A.M. Ibrahim, M. Messali, Z. Moussa, A.Y. Alzahrani, S.N. Alamry, B. Hammouti, *Portug. Electrochim. Acta*, 29 (2011) 375-389.
59. A. Guendouz, N. Missoum, A. Chetouani, S.S. Al-Deyab, B. Ben Cheikhe, N. Boussalah, B. Hammouti, M. Taleb, A. Aouniti, *Intern. J. ELectrochem. Sci.*, 8 (2013) 4305-4327.
60. A. Ghazoui, N. Bencaht, S.S. Al-Deyab, A. Zarrouk, B. Hammouti, M. Ramdani, M. Guenbour, *Intern. J. ELectrochem. Sci.*, 8 (2013) 2272-2292.
61. J. Haque, K.R. Ansari, V. Srivastava, M.A. Quraishi, I.B. Obot, *Journal of Industrial and Engineering Chemistry*, 49 (2017) 176-188.
62. W. Zhang, R. Ma, H. Liu, Y. Liu, S. Li, L. Niu, *J. Mol. Liq.*, 222 (2016) 671-679.
63. V.V. Torres, V.A. Rayol, M. Magalhães, G.M. Viana, L.C.S. Aguiar, S.P. Machado, H. Orofino, E. D'Elia, *Corros. Sci.*, 79 (2014) 108-118.
64. M.I. Awad, *J. Appl. Electrochem.*, 36 (2006) 163.
65. D.F. Roeper, D. Chidambaram, C.R. Clayton, G.P. Halada, *Electrochim. Acta*, 53 (2008) 2130-2134.
66. E.E. Oguzie, Y. Li, F.H. Wang, *Electrochim. Acta*, 53 (2007) 909-914